

Communication-Efficient Distributed Cooperative Learning with Compressed Beliefs

Mohammad Taha Toghani, César A. Uribe

Department of Electrical and Computer Engineering, Rice University, Houston, TX, USA

{mttoghani, cauribe}@rice.edu

Abstract—We study the problem of distributed cooperative learning, where a group of agents seek to agree on a set of hypotheses that best describes a sequence of private observations. In the scenario where the set of hypotheses is large, we propose a belief update rule where agents share compressed (either sparse or quantized) beliefs with an arbitrary positive compression rate. Our algorithm leverages a unified and straightforward communication rule that enables agents to access wide-ranging compression operators as black-box modules. We prove the almost sure asymptotic exponential convergence of beliefs around the set of optimal hypotheses. Additionally, we show a non-asymptotic, explicit, and linear concentration rate in probability of the beliefs on the optimal hypothesis set. We provide numerical experiments to illustrate the communication benefits of our method. The simulation results show that the number of transmitted bits can be reduced to 5–10% of the non-compressed method in the studied scenarios.

Index Terms—Distributed algorithms, compressed communication, algorithm design and analysis, Bayesian update.

I. INTRODUCTION

During the past decade, the analysis of distributed systems has seen a dramatic rise in interest. Fundamental limitations and structural properties of distributed systems such as limited memory, communication bandwidth, and lack of a central coordinator require coordination by distributed information sharing. Analysis of social networks as well as sensor networks [1]–[4], distributed inference and estimation [5]–[7], and multi-agent control [8], [9] are all among common applications of distributed learning.

We consider the problem of decision making in a network, where agents observe a stream of private signals and exchange their beliefs to agree on a hypothesis that best describes the statistical model of their observations. Fully Bayesian solutions require agents to have rather a complete knowledge of the full distributed system, such as each other’s likelihood functions [10], [11]. On the other hand, locally Bayesian (i.e., non-Bayesian) approaches [12]–[14] alternatively suggest agents to (i) update their beliefs internally using the Bayes rule and (ii) combine their beliefs locally among neighbors using a fusion rule.

Conventional non-Bayesian algorithms require agents to share their beliefs on all hypotheses with their neighbors [4], [14], [15]. However, this imposes large communication loads shall the set of hypotheses is large. In such cases, it may not be necessary that agents exchange all their beliefs with each other. Instead, a compressed version of beliefs could be shared through the network [16]–[18].

Works in [16] and [17] propose algorithms with a compressed message sharing with the assumption of a unique common parameter locally optimal for all agents. Furthermore, these algorithms consider unweighted graphs for the communication besides specific sparsification and quantization methods. More importantly, no non-asymptotic analysis is available even under those stronger assumptions. In this paper, we work with milder assumptions such as weighted networks and conflicting hypotheses, i.e., the set of parameters that best describes all agents’ observations (on average) may not be locally optimal for all agents. We furthermore seek to provide the first non-asymptotic analysis for non-Bayesian learning with compressed communication. Besides, our algorithm provides a unified framework that accommodates a wide range of compression operators (Section II). In [18], authors study the possibility of answering binary questions about a particular hypothesis by sending a subset of beliefs. They propose an algorithm with partial information sharing to reduce communication. In contrast, we will present a more general approach that contains various quantization and sparsification operators.

This paper proposes a distributed non-Bayesian algorithm for social learning where agents exchange their compressed beliefs. The core of our algorithm is inspired by CHOCO-GOSSIP [19, Algorithm 1], but we develop a modified version of their results to show convergence in our algorithm. Our algorithm inherits CHOCO’s benefits like arbitrary compression rate and mild assumptions on the quantizer.

The contributions of this paper are threefold:

- We propose a novel algorithm for non-Bayesian distributed learning with (possibly) arbitrary compressed communication per round. Our algorithm follows a unified consensus mechanism covering a wide range of compression operators, including both sparsification and quantization functions. Thus, it provides a simple and general communication rule for agents to leverage a proper compression operator as a black-box module. We also show a memory-efficient version of the algorithm.
- We provide a non-asymptotic, explicit, and linear convergence rate of beliefs for our algorithm in probability. We work under the conflicting hypotheses setup, where optimal hypotheses of each agent locally need not be the optimal hypotheses of the network. We also prove exponential asymptotic convergence of the beliefs around the set of optimal hypotheses almost surely.
- Finally, we show the communication advantages of our algorithm through extensive numerical experiments on

various compression operators as well as multiple network topologies. We also consider the problem of distributed source localization in a 3D space and explore the application of our method in this problem.

The remainder of this paper is organized as follows. In Section II, we describe the problem and state our main algorithm and results. In Section III, we prove the almost sure asymptotic exponential convergence rate for the proposed algorithm. Likewise, we provide the non-asymptotic convergence rate in probability for our algorithm in Section IV. In Section V, we illustrate the proposed algorithm via numerical experiments. Finally, we end with concluding remarks and discussing future works in Section VI.

Notation: We write $[n]$ to denote the set $\{1, \dots, n\}$. We use the notation of bolding for vectors and matrices. For a matrix $\mathbf{A} \in \mathbb{R}^{n \times n}$, we write $[\mathbf{A}]_{ij}$ or \mathbf{A}_{ij} to denote the entry in the i -th row and j -th column. We use \mathbf{I}_n for the identity matrix of size $n \times n$ as well as $\mathbf{1}_n$ for the vector of all one with size n where we drop the subscript for brevity. We refer to agents and time by subscripts and superscripts, respectively. We write $\lambda_i(\mathbf{A})$ to denote the i -th eigenvalue of matrix \mathbf{A} in terms of magnitude where $|\lambda_1(\mathbf{A})| \geq |\lambda_2(\mathbf{A})| \geq \dots \geq |\lambda_n(\mathbf{A})|$. For arbitrary vectors $\mathbf{x}, \mathbf{y} \in \mathbb{R}^n$, $\log \mathbf{x}$, $\mathbf{x} \cdot \mathbf{y}$, and \mathbf{x}/\mathbf{y} denote element-wise log, product, and division, respectively. $\|\mathbf{x}\|$ stands for 2-norm of vector \mathbf{x} . We denote $\mathcal{N}_c(g, \sigma^2)$ as a truncated Gaussian distributions with mean g , variance σ^2 and cut-off points $\{g \pm c\}$.

II. PROBLEM SETUP AND MAIN RESULTS

We begin with the description of the communication network and non-Bayesian learning problem. Then, we state the corresponding optimization formulation and discuss its properties. We also explain the properties of our desired compression operators and introduce some examples that satisfy those properties. Further, we present our algorithm and provide a detailed explanation for it. Finally, we present our two main theorems (asymptotic and non-asymptotic convergence) and the assumption that guarantees our results.

Communication Network: We consider a group of n agents interacting over an undirected connected communication network $\mathcal{G} = \{\mathcal{V}, \mathcal{E}\}$ where $\mathcal{V} = [n]$ and \mathcal{E} represent the set of agents and edges, respectively. The corresponding adjacency matrix, $\mathbf{A} \in [0, 1]^{n \times n}$, is symmetric (i.e., $\mathbf{A} = \mathbf{A}^\top$) and doubly stochastic (i.e., $\mathbf{A}\mathbf{1} = \mathbf{A}^\top\mathbf{1} = \mathbf{1}$), where $\mathbf{A}_{ij} = 0$ for $(i, j) \notin \mathcal{E}$. We know that $1 = |\lambda_1(\mathbf{A})| > |\lambda_2(\mathbf{A})|$, thus the spectral gap of \mathbf{A} , indicated by $\delta \triangleq 1 - |\lambda_2(\mathbf{A})|$ lies in interval $(0, 1]$. Moreover, we denote $\beta \triangleq \|\mathbf{I} - \mathbf{A}\|_2 \in [0, 2]$. Figure 1 for example shows a communication network of three agents with $\delta \approx 0.24$, $\beta \approx 0.76$.

Non-Bayesian Learning: Each agent $i \in [n]$ observes the random variables S_1^i, S_2^i, \dots , which are i.i.d. and distributed according to an unknown distribution f_i . The set of possible outcomes for agent i is indicated by \mathcal{S}_i , i.e., $s_i^t \in \mathcal{S}_i$. We write $\Theta = \{\theta_1, \theta_2, \dots, \theta_m\}$ to denote the set of m parameters with respect to which agent i has a family of probability distributions, namely $\{\ell_i(\cdot|\theta_k)\}_{k=1}^m$. In social learning problems, Θ represents the set of hypotheses where agent i considers

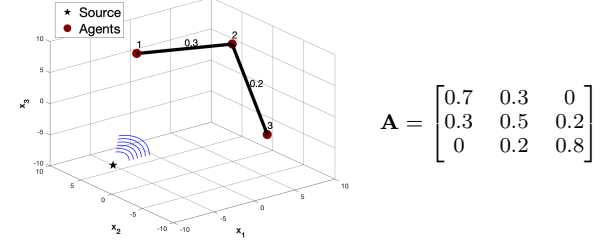


Fig. 1: Distributed Source localization of a group of three agents in a 3D grid of $5 \times 5 \times 5$ hypotheses. The source (shown by star) transmits noisy signals to each agent (sensor) proportional to its corresponding distance. Agents communicate over a path-shaped network with adjacency matrix \mathbf{A} .

$\ell_i(\cdot|\theta_k)$ as the probability distribution corresponding to its observations if θ_k is the true hypothesis. The ultimate goal of agents is to solve the following optimization problem

$$\Theta^* = \arg \min_{\theta \in \Theta} F(\theta) \triangleq \frac{1}{n} \sum_{i=1}^n D_{\text{KL}}(f_i \parallel \ell_i(\cdot|\theta)), \quad (1)$$

where $D_{\text{KL}}(f_i \parallel \ell_i(\cdot|\theta))$ is Kullback-Leibler (KL) divergence between f_i (distribution of S_i^t) and $\ell_i(\cdot|\theta)$, and Θ^* is the set of optimal parameters where $\forall \theta_w \in \Theta^*, F(\theta_w) = F^*$.

Equation (1) is well-defined since it can potentially have multiple answers and does not impose the existence of any θ such that $\ell_i(\cdot|\theta) = f_i$. In other words, this optimization problem seeks to find the parameter(s) $\theta_k \in \Theta$, which best describes all unknown distributions (on average). This formulation also does not require the optimal parameter (on average) to be locally optimal for all agents.

For instance, consider a simple problem of distributed source localization based on differential signal amplitudes [20]. As shown in Fig. 1, let assume that all agents receive noisy signals (with finite support) proportional to their distance from a source with an unknown position. The goal is to identify the source position, approximately. Therefore, each agent builds a 3D grid segmentation $\{-10, -5, 0, 5, 10\}^3$ with $m = 125$ hypotheses as well as corresponding likelihood functions. Let $\mathbf{x}_i, \mathbf{x}_s, \mathbf{x}_{\theta_k} \in \mathbb{R}^3$ respectively be the position of agent $i \in [n]$, source, and our hypothesis $k \in [m]$ for the source. As well, consider truncated zero-mean Gaussian noises with variance σ^2 for the signals, thus $f_i = \mathcal{N}_c(\|\mathbf{x}_i - \mathbf{x}_s\|, \sigma^2)$ and $\ell_i(\cdot|\theta) = \mathcal{N}_{\tilde{c}}(\|\mathbf{x}_i - \mathbf{x}_{\theta}\|, \sigma^2)$, $\forall i \in [n], \forall \theta \in \Theta$. Also, assume that \tilde{c} is set large enough to cover the support of $\mathcal{N}_c(\|\mathbf{x}_i - \mathbf{x}_s\|, \sigma^2)$. The hypotheses with the same distance d from each agent, lie on a circle with radius d and are equally likely to be selected without a cooperative learning process. Note that the number of hypotheses increases exponentially with the dimension and scale of the grid, thus compressed communication is essential. For example, with 1000 partition in each axis, there will be 1000^3 hypotheses. We will provide the result for this example in Section V.

To reach a consensus on the set of optimal hypotheses, each agent builds a probability distribution over Θ , which we refer to as beliefs. Namely $\mu_i^t(\theta)$ stands for agent i 's belief on hypothesis θ at time t that evolves during the

TABLE I: Example compression operators satisfying Eq. (2) and their encoding bits, given b bits baseline for floating-point scalars, m -dimensional vectors, and κ defined in Eq. (3). For rand_k and top_k , $k \in [m]$ indicates the number of coordinates (out of m) being transferred. For $\text{qsgd}_{k-\text{bits}}$, $k \in [b]$ indicates the number of bits by which we quantize each coordinate.

Q operator	type	ω	encoding bits
rand_k	sparsification	k/m	$k(b + \log m)$
top_k	sparsification	k/m	$k(b + \log m)$
$\text{qsgd}_{k-\text{bits}}$	quantization	κ^{-1}	$mk + b$
full	no compression	1	mb

time. We will use the shorthand $\mu_i^t \in \mathbb{R}^m$ as vector $[\mu_i^t(\theta_1), \mu_i^t(\theta_2), \dots, \mu_i^t(\theta_m)]^\top$ as well as similar bold notations from here onwards. Regarding the source localization example, each agent can, for instance, have a uniform initialization on all beliefs, $\mu_i^0(\theta) = 1/125$, when no prior information is available.

Compression: Agents exchange their beliefs of dimension m with each other. Thus, given b bits baseline for a floating-point scalar, they need to send mb bits for each message. We propose to compress messages with a proper algorithm before communication. Here, we introduce a property for our desired compression operators, and then we explain our algorithm.

Following [19], [21], [22], we consider a series of compression operators $Q : \mathbb{R}^m \rightarrow \mathbb{R}^m$ that satisfy

$$\mathbb{E}_Q \|Q(\mathbf{x}) - \mathbf{x}\|^2 \leq (1 - \omega) \|\mathbf{x}\|^2, \quad \forall \mathbf{x} \in \mathbb{R}^m, \quad (2)$$

for a parameter $0 < \omega \leq 1$, which is the desired *compression ratio* and \mathbb{E}_Q indicates the expectation over the internal randomness of operator Q . A wide range of compression operators of both sparsification and quantization functions satisfy Eq. (2), including:

- rand_k or $\text{rand}_{100\omega\%}$: Randomly selecting k out of m coordinates and setting the rest to zero.
- top_k or $\text{top}_{100\omega\%}$: Selecting k out of m coordinates with highest magnitude and setting the rest to zero.
- $\text{qsgd}_{k-\text{bits}}$: Rounding each coordinate of $|\mathbf{x}|/\|\mathbf{x}\|$ to one of the $u = 2^{k-1} - 1$ quantization levels or zero ($k-1$ bits), and one bit for the sign of the coordinate. The quantization operator is defined as follows:

$$Q(\mathbf{x}) = \text{qsgd}_{k-\text{bits}}(\mathbf{x}) = \frac{\text{sign}(\mathbf{x}) \cdot \|\mathbf{x}\|}{u\kappa} \left\lfloor u \frac{|\mathbf{x}|}{\|\mathbf{x}\|} + \zeta \right\rfloor, \\ \text{with } \kappa = (1 + \min \{m/u^2, \sqrt{m}/u\}), \quad (3)$$

where $\zeta \sim_{\text{u.a.r.}} [0, 1]^m$, $\omega = 1/\kappa$, and all operators ($\text{sign}(\cdot)$, $\lfloor \cdot \rfloor$, and products) are element-wise.

Table I summarizes the compression ratio ω and the number of bits required for encoding an m -dimensional message with each of the above three operators. For a more comprehensive list of operators (biased or unbiased), see [22].

Based on what we explained hitherto, we are ready to state our distributed non-Bayesian learning algorithm.

Main Algorithm: In traditional distributed non-Bayesian learning algorithms [1], [15], each agent i updates its beliefs μ_i^{t+1} at time $t+1$ based on: (i) its previous beliefs μ_i^t , (ii) its

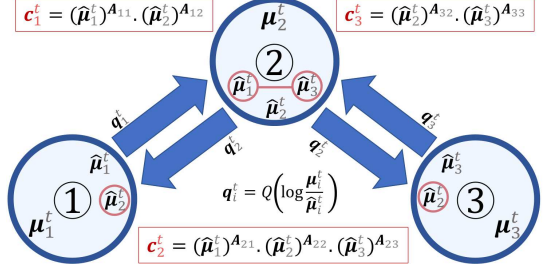


Fig. 2: A group of three agents communicating over a path network. The parameters required in the local memory of each node are shown around it. In accordance with step 7 of Algorithm 1, each node keeps an approximation of its neighbors' beliefs. By replacing the parameters in the red circles with parameters \mathbf{c}_1 , \mathbf{c}_2 , and \mathbf{c}_3 , we can derive a memory-efficient implementation for our algorithm.

new observation s_i^{t+1} , and (iii) its neighbors' previous beliefs $\mu_j^t, \forall (i, j) \in \mathcal{E}$. According to [15, Eq. (2)], each adjacent pair (i, j) exchanges its beliefs on all hypotheses (μ_i, μ_j) per round. Instead, in our approach, every neighbor j of agent i ($\forall (i, j) \in \mathcal{E}$) keeps an approximation of μ_i^t , namely $\hat{\mu}_i^t$. In fact, each agent i communicates the compressed ratio between its recently updated beliefs and their corresponding approximation, thus agent i 's neighbors can combine these compressed vectors to build their approximation of agent i 's beliefs $\hat{\mu}_i^t$, and use it to update their beliefs instead of μ_i^t .

In summary, the following update rule explains our algorithm: $\forall i \in [n], \forall \theta \in \Theta$,

$$\hat{\mu}_i^{t+1}(\theta) = \hat{\mu}_i^t(\theta) \exp \{Q^\theta (\log (\mu_i^t / \hat{\mu}_i^t))\}, \quad (4a)$$

$$\mu_i^{t+1}(\theta) = \mu_i^t(\theta) \prod_{j=1}^n \left(\frac{\hat{\mu}_j^{t+1}(\theta)}{\hat{\mu}_i^{t+1}(\theta)} \right)^{\gamma \mathbf{A}_{ij}} \ell_i(s_i^{t+1} | \theta), \quad (4b)$$

$$\hat{\mu}_i^{t+1}(\theta) = \mu_i^{t+1}(\theta) / \sum_{k=1}^m \mu_i^{t+1}(\theta_k), \quad (4c)$$

where $\hat{\mu}_i^t$ and $\hat{\mu}_i^t$ respectively indicate the approximated and normalized version of μ_i^t with $\hat{\mu}_i^0(\theta) = 1, \forall i \in [n], \forall \theta \in \Theta$. In Eq. (4a), Q^θ indicates the entry corresponding to θ (recall that the output of $Q(\cdot)$ is a vector). Parameter $\gamma \in (0, 1]$ is the stepsize in our algorithm where its value depends on the network topology δ , the number of agents n and beliefs m , and more importantly, the compression ratio ω .

According to Eq. (4a), each agent i computes the difference of its beliefs μ_i^t with its approximation $\hat{\mu}_i^t$ and sends the compression $Q(\log \mu_i^t - \log \hat{\mu}_i^t)$ to all its neighbors. Thus, the number of communicated bits per round can be reduced (roughly) by a factor of ω . Algorithm 1 illustrates the update rule in Eq. (4) in more details. Figure 2 for example portrays the interaction between 3 agents on a path network, where each agent i sends and receives compressed messages and updates the value of $\hat{\mu}_j^t$, $\forall j$ s.t. $(i, j) \in \mathcal{E}$, internally. This procedure is explained in steps 3 to 9 of Algorithm 1. Note that with $\omega = 1$, Eq. (4) turns into [15, Eq. (2)].

Memory-Efficient Algorithm: In Algorithm 1, each agent is required to keep the approximation of all its neighbors'

Algorithm 1 Distributed Non-Bayesian Learning with Compressed Communication

Input: initial beliefs $\mu_i^0 \in \mathbb{R}^m$, communication network \mathbf{A} , compression ratio $\omega \in (0, 1]$, and stepsize $\gamma \in (0, 1]$

Procedure :

```

1: initialize  $\hat{\mu}_i^0 := \mathbf{1}_m$  and  $\tilde{\mu}_i^0 := \mu_i^0 \quad \forall i \in [n]$ 
2: for  $t$  in  $0, \dots, T - 1$ , in parallel  $\forall i \in [n]$  do
3:    $\mathbf{q}_i^t := Q(\log \mu_i^t - \log \hat{\mu}_i^t)$ 
4:   for  $j \in [n]$  such that  $\mathbf{A}_{ij} > 0$  (including  $j = i$ ) do
5:     Send  $\mathbf{q}_i^t$  and receive  $\mathbf{q}_j^t$ 
6:     for  $\theta \in \Theta$ , in parallel do
7:        $\hat{\mu}_j^{t+1}(\theta) = \hat{\mu}_j^t(\theta) \cdot \exp(q_j^t(\theta))$ 
8:     end for
9:   end for
10:  Observe  $s_i^{t+1}$ 
11:  for  $\theta \in \Theta$ , in parallel do
12:     $\mu_i^{t+1}(\theta) = \mu_i^t(\theta) \prod_{j=1}^n \left( \frac{\hat{\mu}_j^{t+1}(\theta)}{\hat{\mu}_i^{t+1}(\theta)} \right)^{\gamma \mathbf{A}_{ij}} \ell_i(s_i^{t+1} | \theta)$ 
13:  end for
14:   $\tilde{\mu}_i^{t+1} = \frac{1}{\mathbf{1}^\top \mu_i^{t+1}} \mu_i^{t+1}$ 
15: end for

```

Output: final beliefs $\tilde{\mu}_i^T \in \mathbb{R}^m \quad \forall i \in [n]$

beliefs locally. Thus, it seems that the memory requirement for each node needs to be proportional to its degree. However, as discussed in [19, Appendix E], a simple memory-efficient implementation can be employed to allocate a common variable to all the approximated beliefs of its neighbors. Specifically, each agent i , can keep three vectors μ_i^t , $\hat{\mu}_i^t$, and $\mathbf{c}_i^t = \prod_{j: \mathbf{A}_{ij} > 0} (\hat{\mu}_j^t)^{\mathbf{A}_{ij}}$ (power and product operators are entrywise), or equivalently $3m$ parameters. Figure 2 illustrates which parameters should be replaced with \mathbf{c}_i^t , for the three agents. A detailed pseudo-code for the efficient implementation is presented in Appendix A.

Next, we state our assumption on the initial conditioning and family of parameterized likelihood of the problem. This will guarantee the convergence properties of our algorithm.

Assumption 1. For all agents $i \in [n]$ and parameters $\theta \in \Theta$, the following properties hold:

- (a) $\exists \alpha_1 > 0$ such that $\mu_i^0(\theta) > \alpha_1$,
- (b) $\exists \alpha_2 > 0$ such that if $f_i(s_i^t) > 0$ then $\ell_i(s_i^t | \theta) > \alpha_2$.

Uniform beliefs on all hypotheses ($\mu_i^0 = \frac{1}{m} \mathbf{1}_m$) not only satisfy Assumption 1(a), but are also reasonable when there is no prior information. Moreover, Assumption 1(b) in addition to having absolutely continuous likelihood functions with respect to f , implies a lower bound in the value of the likelihood functions. This assumption has been used before and it is common in the literature [15], [23].

We now state our first result on the asymptotic convergence of the beliefs generated by Eq. (4). We show that the ratio between the beliefs of any non-optimal and optimal hypotheses decays to zero asymptotically. This in turn implies the concentration of beliefs on the possibly non unique optimal hypothesis almost surely.

Theorem 1 (Asymptotic Convergence). *Let Assumption 1 hold. There exists $\gamma > 0$, such that $\mu_i^t(\theta)$ generated by Eq. (4), has the following property: $\forall i \in [n], \theta_v \notin \Theta^*, \theta_w \in \Theta^*$*

$$\lim_{t \rightarrow \infty} \frac{1}{t} \mathbb{E}_Q \log \frac{\mu_i^t(\theta_v)}{\mu_i^t(\theta_w)} = -C_v \quad \text{a.s.},$$

where $C_v \triangleq F(\theta_v) - F^*$ is a positive constant.

A detailed proof of Theorem 1 is presented in Section III. Note that there are two types of randomness in Theorem 1 where the almost sure addresses the convergence of beliefs, while the expectation points to the randomness of Q . Next, in Corollary 1 we discuss the limiting value of normalized beliefs $\tilde{\mu}_i^t(\theta)$, which converges to zero for any non-optimal hypotheses.

Corollary 1 (Normalized Beliefs). *Under assumptions of Theorem 1, for any hypothesis outside the optimal set ($\forall \theta \notin \Theta^*$), $\tilde{\mu}_i^t(\theta) \rightarrow 0$ in expectation with respect to the randomness of Q . If the optimal hypothesis is a unique θ^* , i.e., $|\Theta^*| = 1$, then $\tilde{\mu}_i^t(\theta^*) \rightarrow 1$.*

Proof. (Corollary 1) Due to $C_v > 0$ in Theorem 1, we have

$$\mathbb{E}_Q \log \tilde{\mu}_i^t(\theta_v) \leq \mathbb{E}_Q \log \frac{\tilde{\mu}_i^t(\theta_v)}{\tilde{\mu}_i^t(\theta_w)} = \mathbb{E}_Q \log \frac{\mu_i^t(\theta_v)}{\mu_i^t(\theta_w)} \Rightarrow \lim_{t \rightarrow \infty} \mathbb{E}_Q \log \tilde{\mu}_i^t(\theta_v) = -\infty,$$

so, in expectation with respect to the randomness of Q , $\tilde{\mu}_i^t(\theta_v) \rightarrow 0$. Moreover, for a unique θ^* , the desired result follows from the fact that $\sum_{k=1}^m \tilde{\mu}_i^t(\theta_k) = 1$. \square

Theorem 1 states asymptotic convergence guarantees. Now, we present our theoretical result regarding the explicit non-asymptotic convergence rate of the update rule in Eq. (4).

Theorem 2 (Non-Asymptotic Convergence Rate). *Let Assumption 1 hold. For an arbitrary $\rho \in (0, 1)$, set $\gamma \triangleq \delta^2 \omega / (32\delta + 2\delta^2 + 8\beta^2 + 4\delta\beta^2 - 8\delta\omega)$. Then, the beliefs $\tilde{\mu}_i^t(\theta)$ generated by Eq. (4c) have the following property: there is an integer $T(\rho)$ such that, with probability at least $1 - \rho$, $\forall t \geq T(\rho)$, we have*

$$\mathbb{E}_Q \log \mu_i^t(\theta_v) \leq -\frac{t}{2} C_1 + C_2 \quad \forall i \in [n], \forall \theta_v \notin \Theta^*,$$

where

$$C_1 \triangleq \min_{\theta_v \notin \Theta^*} (F(\theta_v) - F^*), \quad C_2 \triangleq \frac{162\sqrt{nm}}{\delta^2 \gamma \omega} \log \frac{1}{\alpha},$$

$$\text{and } T(\rho) \triangleq \frac{8}{C_1^2} (\log \alpha)^2 \log \frac{1}{\rho},$$

with $\alpha = \min\{\alpha_1, \alpha_2\}$.

We will present a detailed proof of Theorem 2 in Section IV. Theorem 2 states an explicit linear rate in terms of t , by providing a probabilistic upper-bound on the expectation of logarithm of beliefs outside the optimal set. In other words, for an arbitrary $\epsilon > 0$, we can compute how large t should be to ensure that $\mathbb{E}_Q \log \mu_i^t(\theta_v)$ is bounded by $\log \epsilon$ with probability at least $1 - \rho$. One should keep in mind that C_1 , $T(\rho)$, and particularly C_2 , all take conservative values. We will see in Section V that Eq. (4) has fast convergence in practice.

III. ASYMPTOTIC CONVERGENCE ANALYSIS

In this section, we prove our result in Theorem 1. We first build an update rule $\nu_i^t(\theta)$ without compression and show that $\mu_i^t(\theta)$ converges to the same value as of $\nu_i^t(\theta)$. So, consider the following update rule

$$\hat{\nu}_i^{t+1}(\theta) = \nu_i^t(\theta), \quad (5a)$$

$$\nu_i^{t+1}(\theta) = \nu_i^t(\theta) \prod_{j=1}^n \left(\frac{\hat{\nu}_j^{t+1}(\theta)}{\hat{\nu}_i^{t+1}(\theta)} \right)^{\gamma \mathbf{A}_{ij}} \ell_i(s_i^{t+1}|\theta), \quad (5b)$$

which is an update rule without compression. Equation (5b) can be simplified using Eq. (5a), as follows:

$$\nu_i^{t+1}(\theta) = \prod_{j=1}^n \nu_j^t(\theta)^{\mathbf{B}_{ij}} \ell_i(s_i^{t+1}|\theta), \quad (6)$$

where $\mathbf{B} \triangleq (1-\gamma)\mathbf{I} + \gamma\mathbf{A}$ is also a doubly stochastic matrix. By construction, we initialize $\nu_i^0(\theta) = \mu_i^0(\theta)$, $\forall i \in [n]$, $\forall \theta \in \Theta$. So, following the proof for [15, Theorem 1] (without normalization), we can conclude that, $\forall i \in [n]$, $\theta_v \notin \Theta^*, \theta_w \in \Theta^*$,

$$\lim_{t \rightarrow \infty} \frac{1}{t} \log \frac{\nu_i^t(\theta_v)}{\nu_i^t(\theta_w)} = -C_v \quad \text{a.s.}, \quad (7)$$

where C_v is same as that of stated in Theorem 1. Further, let define $\xi_i^t(\theta) = \log(\nu_i^t(\theta)/\nu_i^{t-1}(\theta))$ as the ratio of each belief for two subsequent steps. As we mentioned earlier ξ_i^t indicates the vector of $[\xi_i^t(\theta_1), \dots, \xi_i^t(\theta_m)]^\top$. The following lemma provides an upper bound for $\|\xi_i^t\|$.

Lemma 1 (Bounded ratio). *Let Assumption 1 hold and $\alpha = \min\{\alpha_1, \alpha_2\}$. The $\nu_i^t(\theta)$ generated by Eq. (6) has the following property:*

$$\sum_{i=1}^n \|\xi_i^t\|^2 < R^2, \quad t = 1, 2, \dots,$$

where $R \triangleq 4\sqrt{nm}/(\gamma\delta) \log(1/\alpha)$.

Proof. (Lemma 1) Let $\mathcal{L}_i^t(\theta) = \log(\ell_i(s_i^{t+1}|\theta)/\ell_i(s_i^t|\theta))$ be likelihood ratio of two consecutive observations. Also, we define vectors $\xi^t(\theta) = [\xi_1^t(\theta), \xi_2^t(\theta), \dots, \xi_n^t(\theta)]^\top$ and $\mathcal{L}^t(\theta) = [\mathcal{L}_1^t(\theta), \mathcal{L}_2^t(\theta), \dots, \mathcal{L}_n^t(\theta)]^\top$. According to Eq. (6):

$$\begin{aligned} \xi^{t+1}(\theta) &= \mathbf{B}\xi^t(\theta) + \mathcal{L}^t(\theta) \\ &= \mathbf{B}^t\xi^1(\theta) + \sum_{r=1}^t \mathbf{B}^{t-r} \mathcal{L}^r(\theta) \\ &= \mathbf{B}^t\xi^1(\theta) + \sum_{r=1}^t \left(\mathbf{B}^{t-r} - \frac{1}{n}\mathbf{1}\mathbf{1}^\top \right) \mathcal{L}^r(\theta) \\ &\quad + \frac{1}{n}\mathbf{1}\mathbf{1}^\top \sum_{r=1}^t \mathcal{L}^r(\theta), \quad \forall \theta \in \Theta. \end{aligned}$$

First notice that by Eq. (6), the following relation holds:

$$\xi_i^1(\theta) = \log \frac{\nu_i^1(\theta)}{\nu_i^0(\theta)} = \sum_{j=1}^n \mathbf{B}_{ij} \log \frac{\nu_j^0(\theta)}{\nu_i^0(\theta)} + \ell_i(s_i^1|\theta),$$

where for all $i, j \in [n]$, $|\log(\nu_i^0(\theta)/\nu_j^0(\theta))| \leq \log(1/\alpha_1)$ by Assumption 1(a). Similarly, for all $t_1, t_2 \geq 0$, we know

that $|\log(\ell_i(s_i^{t_1}|\theta)/\ell_i(s_i^{t_2}|\theta))| \leq \log(1/\alpha_2)$ by Assumption 1(b). Thus, we can infer that

$$\|\xi^1(\theta)\| \leq \sqrt{n} \log \frac{1}{\alpha_1 \alpha_2} \leq 2\sqrt{n} \log \frac{1}{\alpha}, \quad (8)$$

where the second inequality holds since $\alpha = \min\{\alpha_1, \alpha_2\}$. Also, by definition of $\mathcal{L}_i^t(\theta)$, we have

$$\sum_{r=1}^t \mathcal{L}_i^r(\theta) = \sum_{r=1}^t \log \frac{\ell_i(s_i^{r+1}|\theta)}{\ell_i(s_i^r|\theta)} = \log \frac{\ell_i(s_i^{t+1}|\theta)}{\ell_i(s_i^1|\theta)},$$

therefore, it holds that

$$\max \left\{ \|\mathcal{L}^r(\theta)\|, \left\| \sum_{r=1}^t \mathcal{L}^r(\theta) \right\| \right\} \leq \sqrt{n} \log \frac{1}{\alpha_2} \leq \sqrt{n} \log \frac{1}{\alpha}. \quad (9)$$

Further, recall that $\mathbf{B} = (1-\gamma)\mathbf{I} + \gamma\mathbf{A}$. Then, the spectral gap of \mathbf{B} is equal to $\gamma\delta$, and from [19, Lemma 16] we know that

$$\left\| \mathbf{B}^k - \frac{1}{n}\mathbf{1}\mathbf{1}^\top \right\| \leq (1-\gamma\delta)^k,$$

which helps us to show that

$$\begin{aligned} \left\| \sum_{r=1}^t \left(\mathbf{B}^{t-r} - \frac{1}{n}\mathbf{1}\mathbf{1}^\top \right) \mathcal{L}^r(\theta) \right\| &\leq \sum_{r=1}^t (1-\gamma\delta)^{t-r} \|\mathcal{L}^r(\theta)\| \leq \\ \frac{(1-(1-\gamma\delta)^t)}{\gamma\delta} \sqrt{n} \log \frac{1}{\alpha_2} &\leq \frac{\sqrt{n}}{\gamma\delta} \log \frac{1}{\alpha}. \end{aligned} \quad (10)$$

Using the triangle inequality along with referring to Eq. (8), Eq. (9), and Eq. (10), we finally have the following result:

$$\begin{aligned} \|\xi^{t+1}(\theta)\| &\leq \|\mathbf{B}^t \xi^1(\theta)\| + \left\| \frac{1}{n}\mathbf{1}\mathbf{1}^\top \sum_{r=1}^t \mathcal{L}^r(\theta) \right\| \\ &\quad + \left\| \sum_{r=1}^t \left(\mathbf{B}^{t-r} - \frac{1}{n}\mathbf{1}\mathbf{1}^\top \right) \mathcal{L}^r(\theta) \right\| \\ &\leq \|\xi^1(\theta)\| + \left\| \sum_{r=1}^t \mathcal{L}^r(\theta) \right\| \\ &\quad + \left\| \sum_{r=1}^t \left(\mathbf{B}^{t-r} - \frac{1}{n}\mathbf{1}\mathbf{1}^\top \right) \mathcal{L}^r(\theta) \right\| \\ &\leq \left(3 + \frac{1}{\gamma\delta} \right) \sqrt{n} \log \frac{1}{\alpha} \leq \frac{4\sqrt{n}}{\gamma\delta} \log \frac{1}{\alpha}, \quad \forall \theta \in \Theta, \end{aligned}$$

where by definition of ξ_i^t and $\xi^t(\theta_k)$,

$$\sum_{i=1}^n \|\xi_i^t\|^2 = \sum_{k=1}^m \|\xi^t(\theta_k)\|^2 \leq \frac{16nm}{\gamma^2 \delta^2} (\log \alpha)^2,$$

which is constant and does not depend on t . \square

Further, we state an auxiliary result that will help us prove the compressed communication property of our algorithm. Consider an update rule over $\mathbf{x}_i^t, \hat{\mathbf{x}}_i^t \in \mathbb{R}^m$ with the presence of some exogenous noise $\xi_i^t \in \mathbb{R}^m$

$$\begin{aligned} \hat{\mathbf{x}}_i^{t+1} &= \hat{\mathbf{x}}_i^t + Q(\mathbf{x}_i^t - \hat{\mathbf{x}}_i^t + \xi_i^t) - \xi_i^t, \\ \mathbf{x}_i^{t+1} &= \mathbf{x}_i^t + \gamma \sum_{j=1}^n \mathbf{A}_{ij}(\hat{\mathbf{x}}_j^{t+1} - \hat{\mathbf{x}}_i^{t+1}), \end{aligned} \quad (11)$$

where $\hat{\mathbf{x}}_i^0 = \mathbf{0}, \forall i \in [n]$. Let $\bar{\mathbf{x}}^t$ be the average consensus at round t , i.e., $\frac{1}{n} \sum_{i=1}^n \mathbf{x}_i^t$. Let matrix $\mathbf{X}^t \in \mathbb{R}^{n \times m}$ represents $[\mathbf{x}_1^t, \mathbf{x}_2^t, \dots, \mathbf{x}_n^t]^\top$. Similarly, we denote $\hat{\mathbf{X}}^t = [\hat{\mathbf{x}}_1^t, \hat{\mathbf{x}}_2^t, \dots, \hat{\mathbf{x}}_n^t]^\top$, $\bar{\mathbf{X}}^t = [\bar{\mathbf{x}}^t, \dots, \bar{\mathbf{x}}^t]^\top$, and $\mathbf{Z}^t = [\xi_1^t, \xi_2^t, \dots, \xi_n^t]^\top$. Thus, the update rule in Eq. (11) can be written in the following matrix-wise format:

$$\begin{aligned}\hat{\mathbf{X}}^{t+1} &= \hat{\mathbf{X}}^t + Q \left(\mathbf{X}^t - \hat{\mathbf{X}}^t + \mathbf{Z}^t \right) - \mathbf{Z}^t, \\ \mathbf{X}^{t+1} &= \mathbf{X}^t + \gamma (\mathbf{A} - \mathbf{I}) \hat{\mathbf{X}}^{t+1},\end{aligned}\quad (12)$$

where $Q(\cdot)$ addresses columns of the matrix. Also, $\bar{\mathbf{X}}^t = \frac{1}{n} \mathbf{1} \mathbf{1}^\top \mathbf{X}^t$ by definition. Hence, due to the fact that $\frac{1}{n} \mathbf{1} \mathbf{1}^\top (\mathbf{A} - \mathbf{I}) = \mathbf{0}$ and the consensus rule in Eq. (12), we can conclude that $\bar{\mathbf{X}}^{t+1} = \bar{\mathbf{X}}^t$. Thus, a fixed average during the time, namely $\bar{\mathbf{x}}^t = \bar{\mathbf{x}}$. The following lemma describes the behaviour of the update rule in Eq. (11).

Lemma 2 (A variation of Theorem 2 from [19]). *The update rule in Eq. (11), has the following property:*

$$e_t \leq \left(1 - \frac{\delta^2 \omega}{164} \right) e_{t-1} + L z_t,$$

when using the stepsize $\gamma \triangleq \frac{\delta^2 \omega}{32\delta + 2\delta^2 + 8\beta^2 + 4\delta\beta^2 - 8\delta\omega}$, where $e_t \triangleq \mathbb{E}_Q \sum_{i=1}^n \left(\|\mathbf{x}_i^t - \bar{\mathbf{x}}\|^2 + \|\mathbf{x}_i^t - \hat{\mathbf{x}}_i^{t+1}\|^2 \right)$, $z_t \triangleq \sum_{i=1}^n \|\xi_i^t\|^2$, and $L \triangleq (1 - \omega)(2 - \omega)/\omega$.

The key difference between Lemma 2 and [19, Theorem 2] is the existence of noise signals ξ_i^t in Eq. (11), thus a slight difference in the upper bounds proposed in their results. The proof for Lemma 2 is provided in Appendix B.

Now, we are ready to prove Theorem 1.

Proof. (Theorem 1)

For each hypothesis θ , we divide Eq. (4a) and Eq. (4b) respectively by Eq. (5a) and Eq. (5b), and take logarithm of the result, therefore

$$\begin{aligned}\log \frac{\mu_i^{t+1}}{\nu_i^{t+1}} &= \log \frac{\mu_i^t}{\nu_i^t} + \gamma \sum_{j=1}^n \mathbf{A}_{ij} \left(\log \frac{\hat{\mu}_j^{t+1}}{\hat{\nu}_j^{t+1}} - \log \frac{\hat{\mu}_i^{t+1}}{\hat{\nu}_i^{t+1}} \right), \\ \log \frac{\hat{\mu}_i^{t+1}}{\hat{\nu}_i^{t+1}} &= \log \frac{\hat{\mu}_i^t}{\hat{\nu}_i^t} + \log \frac{\hat{\nu}_i^t}{\hat{\nu}_i^{t+1}} \\ &\quad + Q \left(\log \frac{\mu_i^t}{\nu_i^t} - \log \frac{\hat{\mu}_i^t}{\hat{\nu}_i^t} + \log \frac{\hat{\nu}_i^{t+1}}{\hat{\nu}_i^t} \right),\end{aligned}\quad (13)$$

where all fractions are entrywise divisions as mentioned beforehand. Naming $x_i^t(\theta) = \log(\mu_i^t(\theta)/\nu_i^t(\theta))$ and $\hat{x}_i^t(\theta) = \log(\hat{\mu}_i^t(\theta)/\hat{\nu}_i^t(\theta))$, Eq. (13) turns into Eq. (11). Hence, in line with Lemma 2, we know that $\eta = 1 - (\delta^2 \omega / 164) \in [0, 1]$. Furthermore, Lemma 1 tells us that z_t is bounded by R^2 , thus

$$e_t \leq \eta^t e_0 + L \sum_{k=1}^t \eta^{t-k} z_k \leq \eta^t e_0 + \frac{LR^2(1 - \eta^t)}{1 - \eta}, \quad (14)$$

where dividing by t^2 , we can derive

$$\begin{aligned}\mathbb{E}_Q \left\| \frac{1}{t} (\mathbf{x}_i^t - \bar{\mathbf{x}}) \right\|^2 &\leq \frac{e_t}{t^2} \leq \frac{1}{t^2} \left(\eta^t e_0 + \frac{LR^2(1 - \eta^t)}{1 - \eta} \right) \Rightarrow \\ \lim_{t \rightarrow \infty} \left\| \frac{1}{t} (\mathbf{x}_i^t - \bar{\mathbf{x}}) \right\| &= 0 \quad \text{a.s. } \forall i \in [n],\end{aligned}\quad (15)$$

where $\bar{\mathbf{x}} = \mathbf{0}$ by proper initialization, $\nu_i^0(\theta) = \mu_i^0(\theta), \forall i \in [n]$ and $\forall \theta \in \Theta$. Equation (15) suggests L^2 convergence where replacing \mathbf{x}_i^t with its equivalent expression (entrywise) we have $\mathbb{E}_Q \left\| \frac{1}{t} \log \frac{\mu_i^t(\theta)}{\nu_i^t(\theta)} \right\| \rightarrow 0$. Also, due to the fact that L^2 convergence implies L^1 convergence [24, page 201], i.e., $\mathbb{E}_Q \left| \frac{1}{t} \log \frac{\mu_i^t(\theta)}{\nu_i^t(\theta)} \right| \rightarrow 0$, it is inferred that for any $\epsilon > 0$, there exists a T s.t. $\forall t > T$

$$\left| \mathbb{E}_Q \frac{1}{t} \log \frac{\mu_i^t(\theta)}{\nu_i^t(\theta)} \right| \leq \mathbb{E}_Q \left| \frac{1}{t} \log \frac{\mu_i^t(\theta)}{\nu_i^t(\theta)} \right| < \epsilon, \quad (16)$$

where the first inequality follows Jensen's inequality. We now consider the inequality in Eq. (16) for two arbitrary hypotheses $\theta_v \notin \Theta^*$ and $\theta_w \in \Theta^*$, therefore

$$\begin{aligned}\left| \mathbb{E}_Q \frac{1}{t} \left[\log \frac{\mu_i^t(\theta_v)}{\nu_i^t(\theta_v)} - \log \frac{\mu_i^t(\theta_w)}{\nu_i^t(\theta_w)} \right] \right| &< \\ \left| \mathbb{E}_Q \frac{1}{t} \log \frac{\mu_i^t(\theta_v)}{\nu_i^t(\theta_v)} \right| + \left| \mathbb{E}_Q \frac{1}{t} \log \frac{\mu_i^t(\theta_w)}{\nu_i^t(\theta_w)} \right| &< 2\epsilon,\end{aligned}$$

as a result of triangle inequality. Moreover, as $1/t$ is deterministic, we have

$$\left| \frac{1}{t} \mathbb{E}_Q \log \frac{\mu_i^t(\theta_v)}{\mu_i^t(\theta_w)} - \frac{1}{t} \mathbb{E}_Q \log \frac{\nu_i^t(\theta_v)}{\nu_i^t(\theta_w)} \right| < 2\epsilon,$$

so the two expressions inside the above absolute value converge to each other in limit. Also, from Eq. (7) we know that the second term converges to $-C_v$, therefore

$$\lim_{t \rightarrow \infty} \frac{1}{t} \mathbb{E}_Q \log \frac{\mu_i^t(\theta_v)}{\mu_i^t(\theta_w)} = -C_v,$$

which is our desired result. \square

In the previous result, we show the asymptotic exponential convergence of the ratio between any two non-optimal and optimal hypotheses almost surely. This means that in the limit, the set of optimal hypotheses dominates.

IV. NON-ASYMPTOTIC CONVERGENCE ANALYSIS

In this section, we state a proof for Theorem 2, which provides an explicit convergence rate for our proposed algorithm in Eq. (4). Lemma 3 helps us to connect the convergence of the quantized process to that of the non-quantized process.

Lemma 3 (Variation range). *Let Assumption 1 hold. Further, assume that the update rules in Eq. (4) and Eq. (5) have the same initial values and the stepsize in Theorem 2. Then, for each agent i , parameter $\theta \in \Theta$, and $t = 0, 1, \dots$, the following inequality holds*

$$|\mathbb{E}_Q \log \mu_i^t(\theta) - \log \nu_i^t(\theta)| \leq G_1 \quad \text{const.}$$

where $G_1 = \frac{73\sqrt{nm}}{\delta^2 \gamma \omega} \log \frac{1}{\alpha}$, with $\alpha = \min\{\alpha_1, \alpha_2\}$.

Proof. (Lemma 3) We showed in Eq. (14) that e_t defined in Lemma 2 is bounded. By definition of e_t , \mathbf{x}_i , and the fact that $\bar{\mathbf{x}} = \mathbf{0}$, the following inequality holds

$$\mathbb{E}_Q \|\log \mu_i^t(\theta) - \log \nu_i^t(\theta)\|^2 \leq \mathbb{E}_Q \|\log \mu_i^t - \log \nu_i^t\|^2 \leq \sum_{i=1}^n \mathbb{E}_Q \|\log \mu_i^t - \log \nu_i^t\|^2 \leq e_t \leq \eta^t e_0 + \frac{LR^2(1-\eta^t)}{1-\eta},$$

and by Jensen's inequality, we have

$$\begin{aligned} |\mathbb{E}_Q \log \mu_i^t(\theta) - \log \nu_i^t(\theta)| &\leq \mathbb{E}_Q |\log \mu_i^t(\theta) - \log \nu_i^t(\theta)| \\ &\leq \left(\mathbb{E}_Q |\log \mu_i^t(\theta) - \log \nu_i^t(\theta)|^2 \right)^{\frac{1}{2}}. \end{aligned}$$

It is therefore enough to compute an upper bound for the right-hand side of Eq. (14). Further, $\forall i \in [n]$, $\mu_i^0 = \nu_i^0$, and $\hat{\mu}_i^0 = \mathbf{1}$, so

$$\begin{aligned} e_0 &= \mathbb{E}_Q \sum_{i=1}^n \|\hat{\mathbf{x}}_i^1\|^2 = \mathbb{E}_Q \sum_{i=1}^n \|\log \hat{\mu}_i^1 - \log \hat{\nu}_i^1\|^2 \\ &= \mathbb{E}_Q \sum_{i=1}^n \|Q(\log \mu_i^0) - \log \nu_i^0\|^2 \\ &\leq (1-\omega) \sum_{i=1}^n \|\log \mu_i^0\|^2 \leq (1-\omega) nm (\log \alpha)^2. \end{aligned}$$

Finally, we can conclude that

$$\begin{aligned} \eta^t e_0 + \frac{LR^2(1-\eta^t)}{1-\eta} &\leq e_0 + \frac{LR^2}{1-\eta} < \\ nm (\log \alpha)^2 \left(1 + \frac{2624(1-\omega)(2-\omega)}{\delta^4 \gamma^2 \omega^2} \right) &< \\ \frac{5249}{\delta^4 \gamma^2 \omega^2} nm (\log \alpha)^2 &\Rightarrow \\ |\mathbb{E}_Q \log \mu_i^t(\theta) - \log \nu_i^t(\theta)| &\leq \frac{73\sqrt{nm}}{\delta^2 \gamma \omega} \log \frac{1}{\alpha}. \end{aligned}$$

□

Now, we prove Theorem 2.

Proof. (Theorem 2) By Lemma 3, for a non-optimal hypothesis $\theta_v \in \Theta^*$ and an optimal hypothesis $\theta_w \in \Theta^*$

$$\begin{aligned} \left| \mathbb{E}_Q \log \frac{\mu_i^t(\theta_v)}{\mu_i^t(\theta_w)} - \log \frac{\nu_i^t(\theta_v)}{\nu_i^t(\theta_w)} \right| &\leq \left| \mathbb{E}_Q \log \frac{\mu_i^t(\theta_v)}{\nu_i^t(\theta_v)} \right| \\ &\quad + \left| \mathbb{E}_Q \log \frac{\mu_i^t(\theta_v)}{\nu_i^t(\theta_w)} \right| \leq 2G_1. \end{aligned} \quad (17)$$

Further, by [15, Lemma 10], the following inequality holds:

$$\begin{aligned} \mathbb{E}_S \log \frac{\nu_i^t(\theta_v)}{\nu_i^t(\theta_w)} &\leq \max_i \log \frac{\nu_i^0(\theta_v)}{\nu_i^0(\theta_w)} + \frac{12 \log n}{1-\lambda_2(\mathbf{B})} \log \frac{1}{\alpha_2} \\ &\quad - t \min_{\theta_v \notin \Theta^*} (F(\theta_v) - F^*), \end{aligned}$$

where the expectation \mathbb{E}_S , indicates the randomness of observations. By Assumption 1, $\alpha = \min\{\alpha_1, \alpha_2\}$, and definition of \mathbf{B} , the above inequality can be modified as follows:

$$\mathbb{E}_S \log \frac{\nu_i^t(\theta_v)}{\nu_i^t(\theta_w)} \leq -tC_1 + G_2, \quad (18)$$

where $C_1 = \min_{\theta_v \notin \Theta^*} (F(\theta_v) - F^*)$ and $G_2 = \frac{16 \log n}{\gamma \delta} \log \frac{1}{\alpha}$. On the other hand, we have

$$\mathbb{E}_Q \log \tilde{\mu}_i^t(\theta_v) \leq \mathbb{E}_Q \log \frac{\tilde{\mu}_i^t(\theta_v)}{\tilde{\mu}_i^t(\theta_w)} = \mathbb{E}_Q \log \frac{\mu_i^t(\theta_v)}{\mu_i^t(\theta_w)}, \quad (19)$$

thus the following inequalities hold:

$$\begin{aligned} &\mathbb{P} \left(\mathbb{E}_Q \log \tilde{\mu}_i^t(\theta_v) \geq -\frac{t}{2} C_1 + 2G_1 + G_2 \right) \\ &\leq \mathbb{P} \left(\mathbb{E}_Q \log \frac{\mu_i^t(\theta_v)}{\mu_i^t(\theta_w)} \geq -\frac{t}{2} C_1 + 2G_1 + G_2 \right) \\ &\leq \mathbb{P} \left(\log \frac{\nu_i^t(\theta_v)}{\nu_i^t(\theta_w)} \geq -\frac{t}{2} C_1 + G_2 \right) \\ &\quad + \underbrace{\mathbb{P} \left(\mathbb{E}_Q \log \frac{\mu_i^t(\theta_v)}{\mu_i^t(\theta_w)} \geq \log \frac{\nu_i^t(\theta_v)}{\nu_i^t(\theta_w)} + 2G_1 \right)}_{=0, \text{ by Eq. (17)}} \\ &\leq \mathbb{P} \left(\log \frac{\nu_i^t(\theta_v)}{\nu_i^t(\theta_w)} - \mathbb{E}_S \left[\log \frac{\nu_i^t(\theta_v)}{\nu_i^t(\theta_w)} \right] \geq \frac{t}{2} C_1 \right), \end{aligned}$$

where the first inequality follows Eq. (19), the second inequality is a union bound, and the third inequality holds as a result of Eq. (18). With a similar approach to the proof for [15, Theorem 2], we can use McDiarmid's inequality to bound the above expression by probability ρ . Therefore, $\forall t \geq T(\rho) = \frac{8}{C_1^2} (\log \alpha)^2 \log \frac{1}{\rho}$, with a probability at least $1 - \rho$, the following inequality holds:

$$\mathbb{E}_Q \log \mu_i^t(\theta_v) \leq -\frac{t}{2} C_1 + 2G_1 + G_2 \leq -\frac{t}{2} C_1 + C_2,$$

where $C_2 = \frac{162\sqrt{nm}}{\delta^2 \gamma \omega} \log \frac{1}{\alpha}$. □

We provided a probabilistic finite-time convergence result for our algorithm. The rate of convergence C_1 in our result is same as that of [15, Theorem 2], but the constant C_2 has worse dependencies on parameters n, m, δ . However, we believe the bound is loose, and it can be greatly improved. This remains for future work.

V. NUMERICAL EXPERIMENTS

Our analysis in Section IV suggests that for the beliefs generated by Eq. (4), after a time $T(\rho)$ that depends on the network size and topology, number of beliefs, compression ratio, and initial conditioning of the problem, converges with a linear rate to an optimal solution of Problem in Eq. (1), with a probability of at least $1 - \rho$. In this section, we quantify the performance of our algorithm through a series of empirical experiments. Specifically, we validate the compression capability of our algorithm for various network structures, the number of agents and beliefs, and several compression operator ratios. Finally, we apply our algorithm to 3D source localization (Fig. 1) and explore the effect of the compression ratio in it.

We evaluate our algorithm on path and ring structures with low connectivity (i.e., $\delta^{-1} = \mathcal{O}(n^2)$), as well as Erdős-Rényi (ER), torus, and complete topologies that have higher connectivity. Topologies such as path and ring have mixing times of $O(n^2)$, which increases the message sharing dependency on the number of nodes quadratically. Therefore, the required

number of iterations in such topologies is higher than their dense counterparts like the torus, fully-connected (complete), or expander graphs [25]. The connectivity of Erdős-Rényi graphs depends on their edge probabilities, thus we consider both $p = \log n/n$ and $p = 1/\sqrt{n}$ in our experiments, where the former obviously provides sparser graphs. For a complete list of mixing times, see [25].

Illustrative Experiments: We begin by considering a group of $n = 100$ agents respectively on path, ring, ER- $\log n/n$, torus, ER- $1/\sqrt{n}$, and complete topologies with weights $1/\max\{d^i + 1, d^j + 1\}$ for off-diagonal pairs $(i, j) \in \mathcal{E}$, where d^i is the degree of agent i . We select a large hypothesis set with $m = 400$ as well as a group of observations \mathcal{S}_i with size $|\mathcal{S}_i| = 20$ for each agent i . We also generate a random family of probability distributions, $\{\ell_i(\cdot | \theta_k)\}_{k=1}^m$, as well as a random f_i on each \mathcal{S}_i such that $|\Theta^*| = 1$. The optimal hypothesis is not required to be locally optimal for all agents, by construction.

We first compare the performance of our algorithm using the three compression operators introduced in Table I versus the scenario without any compression [15, Eq. (2)]. We consider the $k = 2$ bits (least precision) and $b = 64$ bits baseline for $\text{qsgd}_{k\text{-bits}}$. According to Eq. (3), this quantization satisfies Eq. (2) with $\omega \approx 0.05$, so we select the other two operators $\text{rand}_{5\%}$ and $\text{top}_{5\%}$ with the same omega. We also consider $\text{top}_{1\%}$ with a lower compression ratio. Under the communication topologies that we explained earlier, we initialize beliefs uniformly and run 5 Monte Carlo runs of Eq. (4). For the choice of γ in all experiments, we apply a grid line search over the set $\{\omega/4, \omega/2, \omega, 2\omega, 4\omega\}$ to pick the value that converges faster in practice. Figure 3 illustrates the result of this experiment, where from the top (path graph) to the bottom (complete graph), the connectivity among agents increases; thus, the spectral gap grows.

In the left-hand plots of Fig. 3, we see the belief evolution of one agent on the optimal hypothesis for different compression operators. In the right-hand plots, we report the convergence error $\frac{1}{n} \sum_{i=1}^n \|\tilde{\mu}_i^t - \mu^*\|$, per the number of transmitted bits, where μ^* is the vector with 1 at the entry corresponding to θ^* and the rest zero. As shown for example in the torus graph results (Fig. 3d), our proposed algorithm requires less communication cost (about 5% – 20% of the full) to reach an $\epsilon = 10^{-5}$ error compared to the algorithm in [15, Eq. (2)]. Nonetheless, the number of iterations required for convergence grows which is an inevitable consequence of arbitrary compression. Further, we can see that $\text{qsgd}_{2\text{bits}}$ converges faster than $\text{top}_{5\%}$, but with decreasing the compression ratio ω to 0.01, the $\text{top}_{1\%}$ achieves a better performance than $\text{qsgd}_{2\text{bits}}$ in terms of the transmitted bits, but requires more iterations to converge (left figures). Complied to our intuition, $\text{qsgd}_{2\text{bits}}$, $\text{top}_{5\%}$, and $\text{top}_{1\%}$ outperform $\text{rand}_{5\%}$ operator.

We further attempt to quantify the mutual effect of the compression ratio ω with the network size n , as well as the hypotheses size m on the convergence rate in Fig. 4 and Fig. 5, respectively. Similar to what we did in the previous experiment, we first fix $m = 400$ and for different network sizes $n \in \{25, 50, 100, 200\}$, we initialize beliefs uniformly and run 5 Monte Carlo

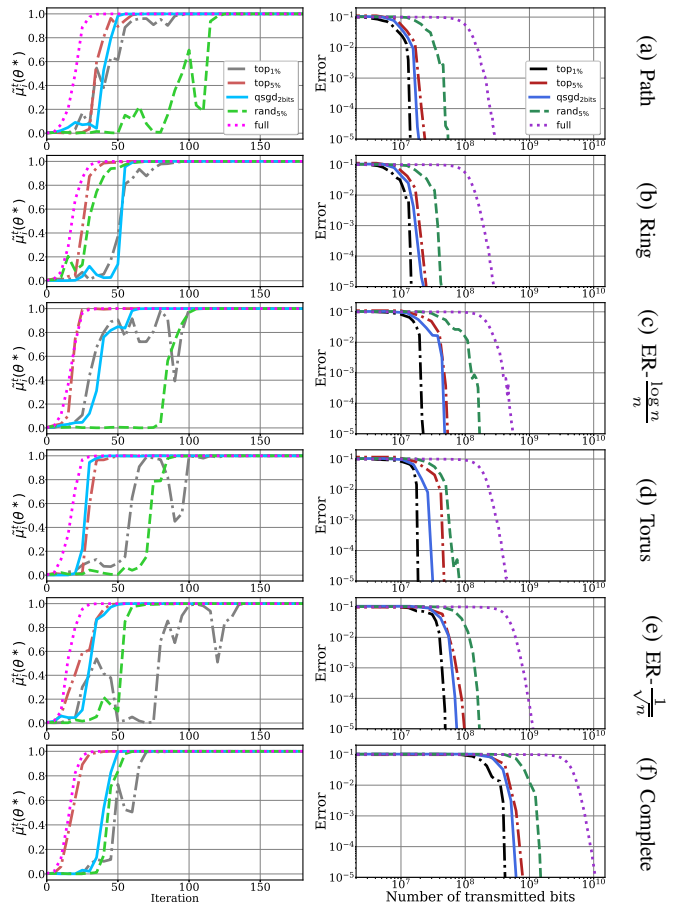


Fig. 3: Each plot is the average of 5 Monte Carlo runs. Convergence of the update rule in Eq. (4) using compression operators in Table I with the update rule in [15, Eq. (2)] over (a) path, (b) ring, (c) Erdős-Rényi with edge probability $p = \log n/n$, (d) torus, (e) Erdős-Rényi with edge probability $p = \sqrt{n}/n$, and (f) complete topologies, with $n = 100$ agents and $m = 400$ hypotheses. In all experiments, γ is chosen by a grid search. **left:** Belief evolution of one agent on the optimal hypothesis. **right:** Convergence error per the number of transmitted bits through the corresponding network.

runs of Eq. (4) with compression operator $\text{top}_{100\omega\%}$ for $\omega \in \{0.0025, 0.005, 0.01, 0.025, 0.05, 0.1, 0.2, 0.5\}$. For the choice of optimal γ we apply a fine geometric grid search.

In the top row of Fig. 4, we see the number of iterations required for agents to reach $\epsilon = 10^{-8}$ accuracy of the optimal hypothesis. In the bottom row, the number of bits required for the same experiments is shown. For example, in Fig. 4b regarding the torus topology, we can see that for different agent numbers n , the number of iterations required for consensus is very similar. In addition, the number of transmitted bits decays to 2.5% with top_1 communication ($\omega = 0.0025$). More importantly, with $\omega = 0.1$, the number of transmitted bits will be decreased to 10% of the full communication with roughly the same number of iterations.

Next, we fix $n = 100$ and for different number of hypotheses $m \in \{100, 200, 500, 100, 2000\}$, we run the same set of experiments. For each m , we consider the set of $\omega \geq 1/m$. In

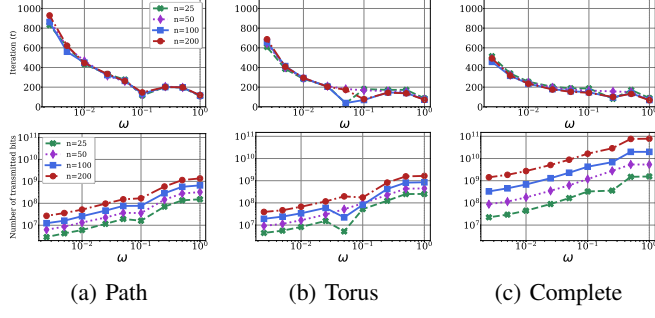


Fig. 4: The empirical mean over 5 Monte Carlo runs of the number of iterations (top) and transmitted bits (bottom), required for $\tilde{\mu}_i^t(\theta) < \epsilon$ for all agents on every $\theta \notin \Theta^*$ with $m = 400$ hypotheses and $\text{top}_{100\omega\%}$ operator over (a) path, (b) torus, and (c) complete topologies. Each line corresponds to a separate value of n for different values of ω .

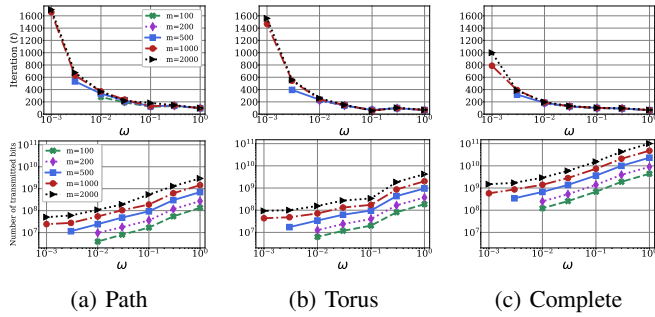


Fig. 5: The empirical mean over 5 Monte Carlo runs of the number of iterations (top) and transmitted bits (bottom), required for $\tilde{\mu}_i^t(\theta) < \epsilon$ for all agents on every $\theta \notin \Theta^*$ with $n = 100$ agents and $\text{top}_{100\omega\%}$ operator over (a) path, (b) torus, and (c) complete topologies. Each line corresponds to a separate value of m for different values of ω .

the top and bottom rows of Fig. 5, the number of iterations and transmitted bits required for ϵ convergence are shown, respectively. In Fig. 5a, we can for example see that for a path graph with $n = 100$ agents and $m = 2000$ hypotheses, the communication cost can be decreased to 2%. Additional results on ring and Erdős-Rényi graphs as well as $\text{qsgd}_{k\text{bits}}$ operator are presented in Appendix C.

Source Localization: As we explained in Section II, consider a group of n agents receiving noisy signals proportional to their distance from a source with an unknown position. To locate the source, each agent divides the space into a grid and builds a set of hypotheses on all hypothetical positions for the source. Using the likelihood model that we explained in Section II, we first apply our algorithm on the setup in Fig. 1. We therefore initialize beliefs uniformly and run 5 Monte Carlo runs of Algorithm 1 using both top_k and qsgd_k compression operators with different compression levels. Figure 6 shows the belief evolution for agent 1 on the closest hypothesis to the source position. We can see that the transmitted bits are decreased to 5–10% compared to [15, Eq. (2)] or $\omega = 1$.

We further investigate the extension of the previous example to larger networks. We consider a group of $n \in \{25, 50, 100\}$

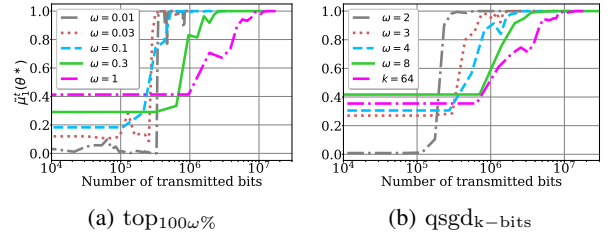


Fig. 6: Each plot is the average of 5 Monte Carlo runs of Eq. (4) on the distributed source localization problem described in Fig. 1. Belief evolution of agent 1 on the optimal hypothesis θ^* (the closest hypothesis to the source) for (a) $\text{top}_{100\omega\%}$ and (b) $\text{qsgd}_{k\text{bits}}$ compression operators with different precision levels.

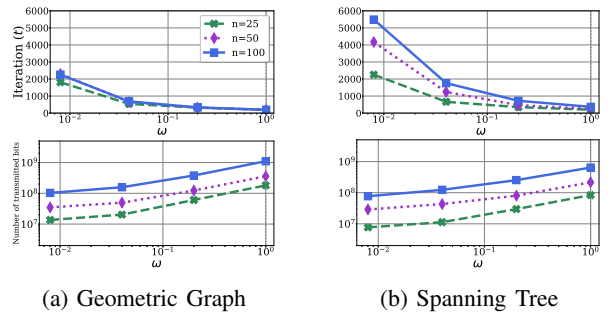


Fig. 7: Each number is the mean over 5 Monte Carlo runs of the corresponding source localization experiment. The number of iterations (top) and transmitted bits (bottom), required for $\tilde{\mu}_i^t(\theta) < \epsilon$ for all agents on every $\theta \notin \Theta^*$ with $m = 125$ hypotheses and $\text{top}_{100\omega\%}$ operator over the (a) geometric and (b) spanning tree topologies. Each line corresponds to a separate value of n .

sensors distributed in the 3D space $[-10, 10]^3$ and seeking to find the position of the source by communicating through their geometric graph [25]. We also choose the minimal spanning tree of these agents as the alternative option for the communication graph with less connectivity. We consider the same $5 \times 5 \times 5$ grid ($m = 125$) and run 5 Monte Carlo runs of our algorithm with compression operator $\text{top}_{100\omega\%}$ for different values of ω under the uniform beliefs initialization and fine-tuned γ . We select $\text{top}_{100\omega\%}$ as the compression operator with different values of ω . Figures 7a and 7b demonstrate the number of iterations as well as the volume of transmitted bits for the ϵ -convergence over the geometric and spanning-tree topologies. The tree topology has a higher mixing time than the geometric graph, thus taking more iterations to converge. Instead, the geometric graph has a slightly higher communication cost. Additional results on a $10 \times 10 \times 10$ grid are presented in Appendix C.

VI. CONCLUSIONS AND FUTURE WORK

We proposed a distributed non-Bayesian update rule where agents exchange compressed messages with an arbitrary compression ratio to reach a consensus [19]. Our algorithm leverages a unified compression mechanism that can embrace a wide range of quantization and/or sparsification operators. Our

main results show that the beliefs generated by our proposed algorithm exponentially concentrates around the set of optimal hypotheses. Furthermore, we presented a probabilistic explicit convergence rate for our method. Finally, we presented empirical evidence suggesting that given a proper compression precision, our algorithm can reduce the required communication load compared to existing approaches (cf. [15]).

Our theoretical analyses and numerical results suggest a strong dependency of convergence rate on the topology of the network. In future work, we will explore how to reduce this dependency. Other aspects of future work would be to use social sampling in the format of compression to provide more comprehensive models for agents' behavior in social networks. Future work should also study the convergence rates for the concentration of beliefs on time-varying and/or directed networks and robustness to stubborn agents.

REFERENCES

- [1] A. Jadbabaie, P. Molavi, A. Sandroni, and A. Tahbaz-Salehi, "Non-Bayesian social learning," *Games and Economic Behavior*, vol. 76, no. 1, pp. 210–225, 2012.
- [2] R. Olfati-Saber, E. Franco, E. Fazzoli, and J. Shamma, "Belief consensus and distributed hypothesis testing in sensor networks," in *Networked Embedded Sensing and Control*, pp. 169–182. Springer, 2006.
- [3] T. Halme, M. Golz, and V. Koivunen, "Bayesian Multiple Hypothesis Testing For Distributed Detection In Sensor Networks," *2019 IEEE Data Science Workshop (DSW)*, pp. 105–109, 2019.
- [4] A. Nedić, A. Olshevsky, and C. Uribe, "Distributed Learning for Cooperative Inference," *ArXiv*, vol. abs/1704.02718, 2017.
- [5] Y. Chen, S. Kar, and J. Moura, "Resilient Distributed Estimation: Sensor Attacks," *IEEE Transactions on Automatic Control*, vol. 64, pp. 3772–3779, 2019.
- [6] S. Al-Sayed, A. Zoubir, and A. Sayed, "Robust Distributed Estimation by Networked Agents," *IEEE Transactions on Signal Processing*, vol. 65, pp. 3909–3921, 2017.
- [7] R. Nassif, S. Vlaski, and A. Sayed, "Distributed Inference over Networks under Subspace Constraints," *ICASSP 2019 - 2019 IEEE International Conference on Acoustics, Speech and Signal Processing (ICASSP)*, pp. 5232–5236, 2019.
- [8] A. Nedić and A. Ozdaglar, "Distributed Subgradient Methods for Multi-Agent Optimization," *IEEE Transactions on Automatic Control*, vol. 54, pp. 48–61, 2009.
- [9] A. Olshevsky, "Linear Time Average Consensus and Distributed Optimization on Fixed Graphs," *SIAM J. Control. Optim.*, vol. 55, pp. 3990–4014, 2017.
- [10] D. Gale and S. Kariv, "Bayesian learning in social networks," *Games and economic behavior*, vol. 45, no. 2, pp. 329–346, 2003.
- [11] D. Acemoglu, M. Dahleh, I. Lobel, and A. Ozdaglar, "Bayesian learning in social networks," *The Review of Economic Studies*, vol. 78, no. 4, pp. 1201–1236, 2011.
- [12] A. Lalitha, T. Javidi, and A. Sarwate, "Social learning and distributed hypothesis testing," *IEEE Transactions on Information Theory*, vol. 64, no. 9, pp. 6161–6179, 2018.
- [13] A. Nedić, A. Olshevsky, and C. Uribe, "Nonasymptotic convergence rates for cooperative learning over time-varying directed graphs," in *2015 American Control Conference (ACC)*. IEEE, 2015, pp. 5884–5889.
- [14] P. Molavi, A. Tahbaz-Salehi, and A. Jadbabaie, "A Theory of Non-Bayesian Social Learning," *Econometrica*, vol. 86, pp. 445–490, 2018.
- [15] A. Nedić, A. Olshevsky, and C. Uribe, "Fast Convergence Rates for Distributed Non-Bayesian Learning," *IEEE Transactions on Automatic Control*, vol. 62, no. 11, pp. 5538–5553, 2017.
- [16] S. Sundaram and A. Mitra, "Distributed Hypothesis Testing and Social Learning in Finite Time with a Finite Amount of Communication," *ArXiv*, vol. abs/2004.01306, 2020.
- [17] A. Mitra, J. Richards, S. Bagchi, and S. Sundaram, "Distributed Inference with Sparse and Quantized Communication," *ArXiv*, vol. abs/2004.01302v3, 2020.
- [18] V. Bordignon, V. Matta, and A. Sayed, "Social Learning with Partial Information Sharing," *ICASSP 2020 - 2020 IEEE International Conference on Acoustics, Speech and Signal Processing (ICASSP)*, pp. 5540–5544, 2020.
- [19] A. Koloskova, S. Stich, and M. Jaggi, "Decentralized Stochastic Optimization and Gossip Algorithms with Compressed Communication," in *International Conference on Machine Learning*, 2019, pp. 3478–3487.
- [20] M. Rabbat and R. Nowak, "Decentralized source localization and tracking [wireless sensor networks]," in *2004 IEEE International Conference on Acoustics, Speech, and Signal Processing*. IEEE, 2004, vol. 3, pp. iii–921.
- [21] D. Alistarh, D. Grubic, J. Li, R. Tomioka, and M. Vojnovic, "Qsgd: Communication-efficient sgd via gradient quantization and encoding," in *Advances in Neural Information Processing Systems*, 2017, pp. 1709–1720.
- [22] D. Kovalev, A. Koloskova, M. Jaggi, P. Richtarik, and S. Stich, "A linearly convergent algorithm for decentralized optimization: Sending less bits for free!," *arXiv preprint arXiv:2011.01697*, 2020.
- [23] S. Boucheron, G. Lugosi, and P. Massart, *Concentration inequalities: A nonasymptotic theory of independence*, Oxford university press, 2013.
- [24] S. Resnick, *A probability path*, Springer, 2019.
- [25] A. Nedić, A. Olshevsky, and C. Uribe, "Graph-theoretic analysis of belief system dynamics under logic constraints," *Scientific reports*, vol. 9, no. 1, pp. 1–16, 2019.

APPENDIX

A. Memory-Efficient Algorithm

Algorithm 2 Memory-Efficient Distributed Non-Bayesian Learning with Compressed Communication

Input: initial beliefs $\mu_i^0 \in \mathbb{R}^m$, communication network \mathbf{A} , compression ratio $\omega \in (0, 1]$, and stepsize $\gamma \in (0, 1]$

Procedure :

- 1: initialize $\hat{\mu}_i^0 := \mathbf{1}_m$, $\mathbf{c}_i^0 := \mathbf{1}_m$, and $\tilde{\mu}_i^0 := \mu_i^0 \quad \forall i \in [n]$
- 2: **for** t in $0, \dots, T-1$, in parallel $\forall i \in [n]$ **do**
- 3: $\mathbf{q}_i^t := Q(\log \mu_i^t - \log \hat{\mu}_i^t)$
- 4: **for** $j \in [n]$ such that $\mathbf{A}_{ij} > 0$ (including $j = i$) **do**
- 5: Send \mathbf{q}_i^t and receive \mathbf{q}_j^t
- 6: **end for**
- 7: Observe s_i^{t+1}
- 8: **for** $\theta \in \Theta$, in parallel **do**
- 9: $\hat{\mu}_i^{t+1}(\theta) = \hat{\mu}_i^t(\theta) \cdot \frac{q_i^t(\theta)}{n}$
- 10: $c_i^{t+1}(\theta) = c_i^t(\theta) \cdot \prod_{j=1}^n q_j^t(\theta)^{\mathbf{A}_{ij}}$
- 11: $\mu_i^{t+1}(\theta) = \mu_i^t(\theta) \cdot \left(\frac{c_i^{t+1}(\theta)}{\hat{\mu}_i^{t+1}(\theta)} \right)^\gamma \cdot \ell_i(s_i^{t+1} | \theta)$
- 12: **end for**
- 13: $\tilde{\mu}_i^{t+1} = \frac{1}{1^\top \mu_i^{t+1}} \mu_i^{t+1}$
- 14: **end for**

Output: final beliefs $\tilde{\mu}_i^T \quad \forall i \in [n]$

B. Proof of Lemma 2

Proof. (Lemma 2) From [19, Lemma 17], we know that

$$\begin{aligned} \|\mathbf{X}^{t+1} - \bar{\mathbf{X}}\|_F^2 &\leq (1 - \gamma\delta)^2 (1 + \tau_1) \|\mathbf{X}^t - \bar{\mathbf{X}}\|_F^2 \\ &\quad + \gamma^2 (1 + \tau_1^{-1}) \beta^2 \|\mathbf{X}^t - \hat{\mathbf{X}}^{t+1}\|_F^2, \end{aligned} \quad (20)$$

so, it is enough to modify [19, Lemma 18] as follows:

$$\begin{aligned} \mathbb{E}_Q \|\mathbf{X}^{t+1} - \hat{\mathbf{X}}^{t+2}\|_F^2 &\leq (1 - \omega) \|\mathbf{X}^{t+1} - \hat{\mathbf{X}}^{t+1} + \mathbf{Z}^{t+1}\|_F^2 \\ &\leq (1 + \tau_0) (1 - \omega) \|\mathbf{X}^{t+1} - \hat{\mathbf{X}}^{t+1}\|_F^2 \\ &\quad + (1 + \tau_0^{-1}) (1 - \omega) \|\mathbf{Z}^{t+1}\|_F^2, \end{aligned} \quad (21)$$

where the second inequality follows [19, Remark 9]. Finally, according to the analysis for [19, Lemma 18], we know that:

$$\begin{aligned} \|\mathbf{X}^{t+1} - \hat{\mathbf{X}}^{t+1}\|_F^2 &\leq \gamma^2 \beta^2 (1 + \tau_2^{-1}) \|\mathbf{X}^t - \bar{\mathbf{X}}\|_F^2 \\ &\quad + (1 + \gamma\beta^2) (1 + \tau_2) \|\mathbf{X}^t - \hat{\mathbf{X}}^{t+1}\|_F^2. \end{aligned} \quad (22)$$

By definition of e_t and Eq. (20), Eq. (21), and Eq. (22), we have

$$\begin{aligned} e_{t+1} &\leq U(\gamma) \|\mathbf{X}^t - \bar{\mathbf{X}}\|_F^2 \\ &\quad + V(\gamma) \|\mathbf{X}^t - \hat{\mathbf{X}}^{t+1}\|_F^2 \\ &\quad + L \|\mathbf{Z}^{t+1}\|_F^2 \\ &\leq \max\{U(\gamma), V(\gamma)\} e_t + L z_t, \end{aligned}$$

where

$$\begin{aligned} U(\gamma) &= (1 - \gamma\delta)^2 (1 + \tau_1) \\ &\quad + (1 + \tau_0) (1 - \omega) \gamma^2 \beta^2 (1 + \tau_2^{-1}), \\ V(\gamma) &= \gamma^2 \beta^2 (1 + \tau_1^{-1}) \\ &\quad + (1 + \tau_0) (1 - \omega) (1 + \gamma\beta)^2 (1 + \tau_2), \\ L &= (1 + \tau_0^{-1}) (1 - \omega), \end{aligned} \quad (23)$$

thus it is enough to select $\gamma, \tau_1, \tau_2, \tau_0$ such that there exists a constant $\eta < 1$, such that

$$\max\{U(\gamma), V(\gamma)\} \leq \eta < 1.$$

So, let fix $\tau_0 \triangleq \frac{\omega}{2(1-\omega)} > 0$, where the fact that $\omega > 0$, guarantees $\tau_0 > 0$. So, we can infer that

$$(1 + \tau_0) (1 - \omega) = 1 - \frac{\omega}{2} = 1 - \hat{\omega},$$

where $\hat{\omega} = \frac{\omega}{2}$. Therefore, parameters in Eq. (23) turns into the following setting:

$$\begin{aligned} U(\gamma) &= (1 - \gamma\delta)^2 (1 + \tau_1) \\ &\quad + (1 - \hat{\omega}) \gamma^2 \beta^2 (1 + \tau_2^{-1}), \\ V(\gamma) &= \gamma^2 \beta^2 (1 + \tau_1^{-1}) \\ &\quad + (1 - \hat{\omega}) (1 + \gamma\beta)^2 (1 + \tau_2), \\ L &= \frac{(1 - \omega)(2 - \omega)}{\omega}, \end{aligned}$$

thus, according to the proof of [19, Theorem 2], for the choice of hyperparameters

$$\begin{aligned} \tau_0 &\triangleq \frac{\omega}{2(1 - \omega)} \\ \tau_1 &\triangleq \frac{\gamma\delta}{2} \\ \tau_2 &\triangleq \frac{\hat{\omega}}{2} = \frac{\omega}{4} \\ \gamma^* &\triangleq \frac{\delta^2 \hat{\omega}}{16\delta + \delta^2 + 4\beta^2 + 2\delta\beta^2 - 8\delta\hat{\omega}} \\ &= \frac{\delta^2 \omega}{32\delta + 2\delta^2 + 8\beta^2 + 4\delta\beta^2 - 8\delta\omega}, \end{aligned}$$

the following statement holds:

$$\begin{aligned} \max\{U(\gamma^*), V(\gamma^*)\} &\leq 1 - \frac{\delta^2 \hat{\omega}}{2(16\delta + \delta^2 + 4\beta^2 + 2\delta\beta^2 - 8\delta\hat{\omega})} \\ &\leq 1 - \frac{\delta^2 \hat{\omega}}{82} = 1 - \frac{\delta^2 \omega}{164}, \end{aligned}$$

thus $\eta \triangleq 1 - \frac{\delta^2 \omega}{164}$. \square

C. Additional Experiments

We present an extensive set of experiments on Fig. 4 and Fig. 5, studying qsgd_{k-bits} compression operator and a few more topologies. Further, we repeat the experiments in Fig 7 for a $10 \times 10 \times 10$ grid.

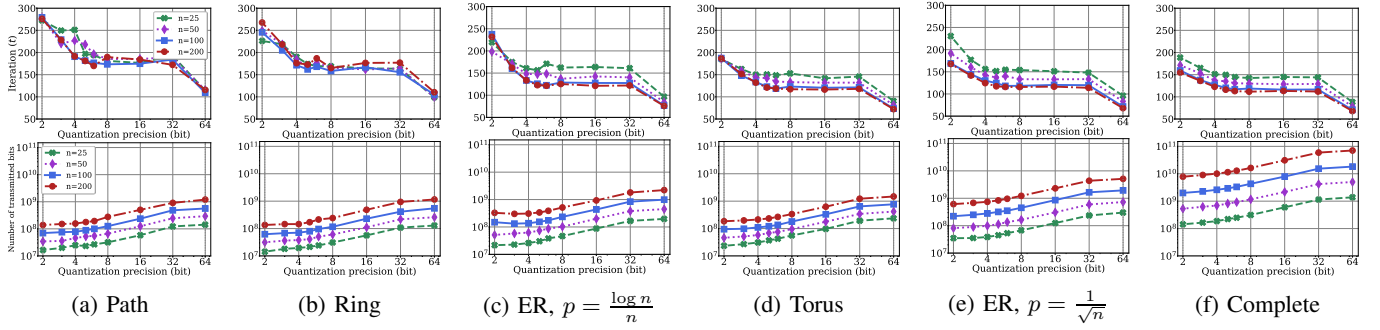


Fig. 8: The same experiments as Fig. 4 on (a) path, (b) ring, (c) ER $p = \log n/n$, (d) torus, (e) ER $p = 1/\sqrt{n}$, and (f) complete topologies with compression operator $\text{qsgd}_{k-\text{bits}}$ for different precision bits k and $b = 64$ baseline bits.

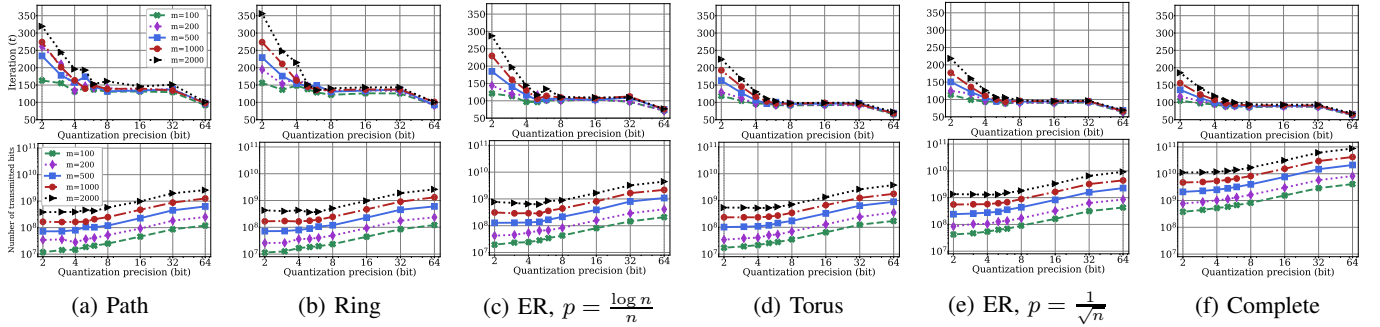


Fig. 9: The same experiments as Fig. 5 on (a) path, (b) ring, (c) ER $p = \log n/n$, (d) torus, (e) ER $p = 1/\sqrt{n}$, and (f) complete topologies with compression operator $\text{qsgd}_{k-\text{bits}}$ for different precision bits k and $b = 64$ baseline bits.

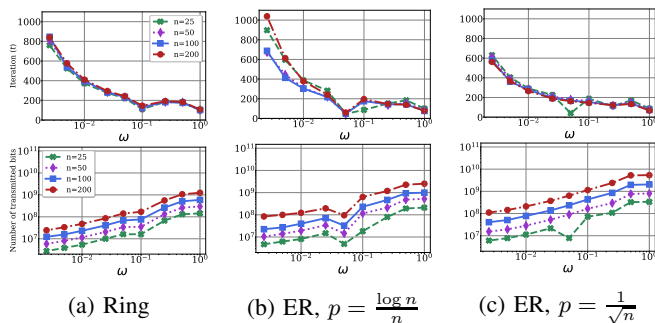


Fig. 10: The same experiments as Fig. 4 on (a) ring, (b) ER $p = \log n/n$, and (c) ER $p = 1/\sqrt{n}$ topologies.

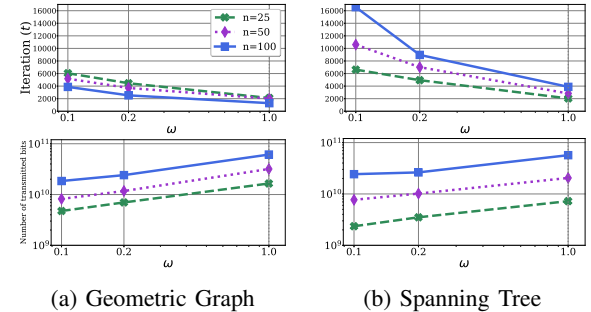


Fig. 12: The same experiments as Fig. 7 on $10 \times 10 \times 10$ grid ($m = 1000$).

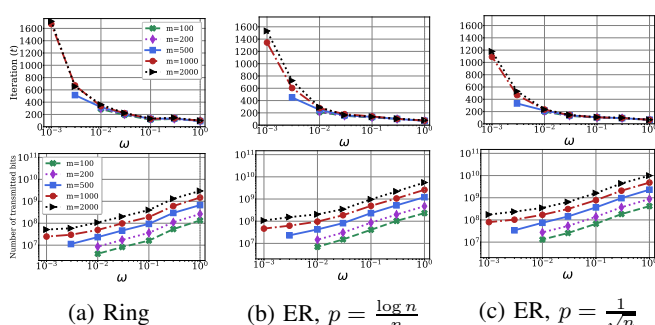


Fig. 11: The same experiments as Fig. 5 on (a) ring, (b) ER $p = \log n/n$, and (c) ER $p = 1/\sqrt{n}$ topologies.

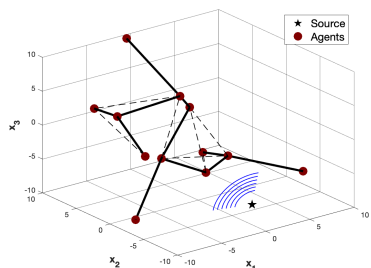


Fig. 13: The setting for the problem of source localization based on differential signal amplitudes for 12 sensors in 3D space $[-10, 10]^3$. The solid lines indicate the edges of the spanning tree connecting the agents. As well, the geometric graph of the agents is shown with solid and dashed edges.